Basil N. Antar, Edwin C. Ethridge, and Daniel Maxwell

Viscosity Measurement using Drop Coalescence in Microgravity

We present in here validation studies of a new method for application in microgravity environment which measures the viscosity of highly viscous undercooled liquids using drop coalescence. The method has the advantage of avoiding heterogeneous nucleation at container walls caused by crystallization of undercooled liquids during processing. Homogeneous nucleation can also be avoided due to the rapidity of the measurement using this method. The technique relies on measurements from experiments conducted in near zero gravity environment as well as highly accurate analytical formulation for the coalescence process. The viscosity of the liquid is determined by allowing the computed free surface shape relaxation time to be adjusted in response to the measured free surface velocity for two coalescing drops. Results are presented from two sets of validation experiments for the method which were conducted on board aircraft flying parabolic trajectories. In these tests the viscosity of a highly viscous liquid, namely glycerin, was determined at different temperatures using the drop coalescence method described in here. The experiments measured the free surface velocity of two glycerin drops coalescing under the action of surface tension alone in low gravity environment using high speed photography. The liquid viscosity was determined by adjusting the computed free surface velocity values to the measured experimental data. The results of these experiments were found to agree reasonably well with the known viscosity for the test liquid used.

1 Introduction

Viscosity is an important thermo-physical property that is used for evaluating the frictional stresses in the liquid and is related to diffusion and reorientational correlation time through the Stokes-Einstein and Debye-Stokes-Einstein relations. Viscosity appears in the classical equations for nucleation and crystal growth by aid of the Stokes-Einstein relation which inversely correlates the viscosity with the diffusion coefficient. The steady state homogeneous nucleation and the crystal growth rate equations used for modeling glass forming liquids, are inversely proportional to the viscosity appearing in the denominator of the pre-exponential term [1,2]. The time for the commencement of nucleation is directly proportional to the viscosity. Viscosity being in the equations is important for order of magnitude calculations of crystalization parameters.

A serious problem with crystallization calculations of many highly undercooled liquids is that viscosity data does not exist between temperatures slightly above the glass transition to just below the melting temperature. Over this temperature range the viscosity can change by as much as 10 orders of magnitude or more. Miani et al. [3] have noted that the problem of having reliable data for the determination of the viscosity (or diffusivity) of highly undercooled liquids has been a serious limitation to the kinetic approach for evaluating the glass forming ability in metallic liquids.

The interpretation of the viscosity of highly undercooled substances is currently limited to fitting of various models to the data. It is almost universally accepted that existing viscosity models are limited and cannot model the entire viscosity range. However, in preliminary studies by Ethridge [4] it has been shown that a number of free volume models of viscosity do provide good fits to the measured data for a wide range of substances over the entire viscosity range. However, the different models can differ by as much as one order of magnitude over the interpolated undercooled region where data is not available. If a single viscosity measurement can be made in the viscosity transition region which currently is inaccessible to direct measurement, then viscosity models can be critically tested. It is to this end that we are developing a low gravity measurement technique for viscosity to be used for liquids in the highly undercooled condition.

The method of drop oscillation in microgravity has been suggested in the past as one technique for determining the viscosi-

Mail address: Prof. Basil N. Antar
MS 26, The University of Tennessee Space Institute
B. H. Goethert Parkway, Tullahoma, TN 37388, USA
Paper submitted: February 25, 2002
Submission of final revised version: April 10, 2002
Paper accepted: April 10, 2002

ty of certain liquids [5]. The method relies on inducing shape oscillations of a spherical drop, using acoustic forcing or other means, and subsequently measuring the decay rate of the oscillation amplitude. The viscosity in this technique is determined through Lamb's formula for the decay rate of the oscillation amplitude in the following manner, [6]:

$$\mu = \frac{\rho R^2}{(l-1)(2l+1)\tau}$$

where ρ, μ and R are the liquid density, viscosity and drop radius, respectively, l is the oscillation mode and τ is the damping time. However, this theory is correct only for liquids possessing weak viscous effects and can not be used for high viscosity liquids such as liquids in the glass transition regime.

It is possible to relax the "small" viscosity values restriction employed in the above expression through the use of extensive numerical computations attempting to fully simulate the oscillation process by solving the complete transient equations of fluid motion for long time periods. There have been a number of numerical studies involving more complicated theory than the use of Lamb's formula. Prosperetti [7] performed calculations involving arbitrary viscosity but considered only small-amplitude oscillations, while Lundgren and Mansour [8] performed calculations for viscous oscillations of small-to-moderate amplitudes and vanishingly small viscosity and inviscid oscillations of large amplitudes. On the other hand, Basaran [9], computed viscous oscillations of large amplitude. All of these analyses, however, considered droplets that were not exposed to any external force field such as gravity or an induced electromagnetic force field commonly used to induce the oscillations, which would incur large errors in the measured value of the viscosity using this method. The forces inducing the oscillations in any experiment can give rise to extremely complicated fluid motion within the drop. Such fluid motion can, in turn, complicate the solution to the equations to such an extent as to make it prohibitive for use for determining the liquid viscosity. In fact, the full transient solution to the equations of motion for an oscillating liquid drop subject to external forcing remains to be performed. This paper discusses an alternative approach in which the free surface energy of the drop is exploited for determining the viscosity of any liquid regardless of its value.

We present in here a novel technique for determining the viscosity of highly viscous liquids using the low gravity environment. The viscosity in this technique is determined simultaneously through detailed measurement as well as numerical simulations of the shape relaxation properties for two merging liquid drops, of the same liquid, under the influence of capillary forces alone. The free surface speed and geometry of the evolving surface during the coalescence of two liquid volumes in zero gravity environment is directly proportional to the liquid viscosity and its surface tension. Thus, when either is known through other means, then the other can be determined from the measured velocity and geometry of the free surface during coalescence. In this paper we show how the viscosity of a liquid can be determined in this manner when its surface tension is known. Eventually, this technique will be applied for conducting accurate measurements of the viscosity of highly undercooled viscous glass melts in the transition region. Traditional terrestrial methods are limited by their contact with container and crucible walls which may cause nucleation in the undercooled melts. On the other hand, container-less measurement methods are limited due to sample deformation in response to large positioning forces, and gravitational body forces that deform the sample shape.

2 Mathematical Model Simulation

The analytical formulation for the problem of liquid coalescence can best be investigated through the solution to the equations of motion for incompressible fluids. Also, since we are interested in the merging of liquid drops under the influence of capillary forces alone, then the equations appropriate for "Stokes" flow can be used for the present simulation. Stoke's equations are derived from the usual momentum equations for incompressible flow in the limit of vanishing inertia force to yeild the following equations:

$$\nabla \cdot \mathbf{u} = 0 \tag{1}$$

$$\mu \nabla^2 \mathbf{u} - \nabla p = 0 \tag{2}$$

where $\mathbf{u} = (u_1, u_2, u_3)$, is the fluid velocity vector field, p is the pressure field inside the liquid mass, ρ is the liquid density, and μ is the liquid dynamic viscosity. This assumption is also true for low Reynolds number flows.

Equations (1) and (2) are linear partial differential equations describing the motion of viscous fluid for creeping flows which is appropriate for the coalescence of two liquid masses such as two liquid drops. Since system (1) and (2) is linear there exists a closed form analytical solution for this system in terms of the *Stokeslets* [10].

In the present simulation we are primarily interested in the merging of two liquid volumes, and specifically, in the free surface evolution as the two volumes merge. This makes the problem essentially a capillary one. Under this condition, the solution to equations (1) and (2) must be consistent with the free surface boundary condition given by the following expression:

$$\mathbf{T} \cdot \mathbf{n} = -\sigma \left(\frac{1}{R_1} + \frac{1}{R_2} \right) \mathbf{n} = \mathbf{b} \tag{3}$$

where $\mathbf{n}$ is the unit normal to the free surface and pointing away from the liquid in this case, σ is the coefficient of surface tension, R_1 and R_2 are the principal radii of curvature of the free surface, and $\mathbf{T}$ is the stress tensor given by the following expression for rectangular Cartesian coordinate system:

$$T_{ij} = -p\delta_{ij} + 2\mu\varepsilon_{ij}\ ,\ \ \varepsilon_{ij} = \frac{1}{2}\left(\frac{\partial u_i}{\partial x_j} + \frac{\partial u_j}{\partial x_i}\right).$$

In order for the drop coalescence problem under investigation to be compatible with anticipated experimental measurements, equations (1) - (3) must be solved in cylindrical or spherical coordinate system. However, in order to demonstrate the solution method adopted here in a clear manner and without the added geometrical complication of the cylindrical coordinate system, the solution method will be first outlined for the geometrically simpler rectangular Cartesian coordinate system. Below we outline the solution procedure for two-dimensional geometry representing the coalescence of two infinitely long circular cylinders.

A. Two-Dimensional Geometry

For the two-dimensional case, the set of governing equations and boundary conditions for the liquid coalescence problem take the following form:

$$\frac{\partial u_1}{\partial x_1} + \frac{\partial u_2}{\partial x_2} = 0 \tag{4}$$

$$\mu\left(\frac{\partial^2 u_1}{\partial x_1^2} + \frac{\partial^2 u_1}{\partial x_2^2}\right) - \frac{\partial p}{\partial x_1} = 0 \tag{5}$$

$$\mu\left(\frac{\partial^2 u_2}{\partial x_1^2} + \frac{\partial^2 u_2}{\partial x_2^2}\right) - \frac{\partial p}{\partial x_2} = 0 \tag{6}$$

$$p - 2\mu\left(\frac{\partial u_1}{\partial x_2} + \frac{\partial u_2}{\partial x_1}\right) = p_0 - \sigma\kappa \tag{7}$$

where κ is the curvature of the free surface curve given by $1/R$ for the two-dimensional case, and p_0 is the pressure of the air surrounding the liquid.

There exists a unique solution for the system (4) - (7) in terms of the fluid velocity field, $\mathbf{u}\{u_1, u_2\}$, given in the following integral form [11]:

$$c_{ij}u_j(x_i) + \int_\Gamma q_{ij}(x_i, y_i)u_j d\Gamma_y = \int_\Gamma s_{ij}(x_i, y_i)b_j d\Gamma_y \tag{8}$$

where in the above y_i is the position vector of the free surface, and x_i is any point in the interior of the liquid mass, (i=1, 2) and (j=1, 2) are the coordinate directions, and

$$c_{ij}\left\{= \delta_{ij}, \mathrm{x} \in \Omega; = \delta_{ij}/2, \mathrm{x} \in \Gamma; = 0, \mathrm{x} \in \Omega'\right\},$$

$$q_{ij}(x_i, y_i) = \frac{r_i r_j}{\pi R^4} r_\kappa n_\kappa$$

$$s_{ij} = \frac{1}{4\pi}\left[\frac{r_i r_j}{R^2} - \delta_{ij}\log R\right]$$

where $r_i = x_i - y_i$, $R = \sqrt{r_1^2 + r_2^2} = |\mathrm{x} - \mathrm{y}|$, and Ω' is the complementary region given by $\Omega \cup \Gamma$. The fluid in this formulation is assumed to be inside the region Ω which is bounded by the curve Γ, and δ_{ij} is the Kronecker delta. The solution given by expression (8) is in a dimensionless form in which the following velocity, pressure, and time scales respectively, have been used:

$$V_s = \sigma/\mu, \quad p_s = \sigma/L, \quad t_s = L\mu/\sigma, \tag{9}$$

L in here is any appropriate length scale, and for the geometry being considered in here could represent the radius of one of the cylinders.

Equation (8) can be cast in the following vector symbolic notation:

$$C\mathbf{u}(\mathbf{x}) + \int_\Gamma Q(\mathbf{x}, \mathbf{y})\mathbf{u}d\Gamma_\eta = \int_\Gamma S(\mathbf{x}, \mathbf{y})\mathbf{b}d\Gamma_\eta \tag{10}$$

where C, Q and S are the second rank tensors whose elements are c_{ij}, q_{ij} and s_{ij}, respectively. In order to ensure a unique solution to this problem, equation (10) must be solved together with the added constraint that the liquid mass must be conserved at the free surface using the following mathematical representation:

$$\int_\Gamma \mathbf{u}d\Gamma = 0\,. \tag{11}$$

Equations (10) and (11) form the basic mathematical model for describing the coalescence process in a two-dimensional Cartesian system. Note that in this form the original differential equation system has been transformed to a system of bounded integral equations in which the free surface is represented by the integration bounds. Such integral formulation for the problem lends itself to a solution through an integral method such as the Finite Element Method (FEM) or the Boundary Element Method (BEM). The BEM is basically a subset of FEM in which only the solution on the boundary of the domain, Γ, is sought while in the FEM the solution is obtained throughout the full domain, Ω, of the problem [12].

Equations (10) and (11) are solved in here using the BEM, which is ideally suited for solving the boundary value problem for the free surface. Also note, that with the BEM method the free surface velocity of the drop, **u**, is the unknown which eliminates the need to ompute the full velocity field within the interior of the drop. Basically, with the BEM, the surface integrations given by equations (10) and (11) are performed by subdividing the surface into discrete segments. This is accomplished by allowing the surface boundary Γ to be discretized into a sequence of boundary curve elements, Γ^i, in which the velocity and surface tension force vectors are written in terms of their values at a sequence of N nodal points along the boundary. Also, with the BEM the surface itself is approximated by a series of simple functions, e.g., linear or quadratic functions through a standard shape function, say Φ, which includes the discrete nodal points on the surface of the fluid volume.

With this process the integral equations (10) and (11) are transformed into a system of N algebraic equations for the N

variables $\mathbf{u}^i$, representing the velocity of each nodal point, i, on the free surface curve Γ. The solution to this system of algebraic equations yields the velocity of the free surface curve as a function of time. Once the velocity of every nodal point is known then the shape evolution of the free surface curve can be constructed using the position of the free surface as a function of time by integrating the following equation at each time step, t:

$$\mathbf{x} = \int \mathbf{u}(\mathbf{x})dt\,. \tag{12}$$

Finally, equation (12) yields the evolution of the geometrical shape of the free surface of the merging liquid drops as a function of time.

A numerical computer code using the BEM was developed along the lines described by van de Vorst et al. [13]. In that code the velocity of each surface element is determined using two-dimensional geometry. For the initial trial validation computations, linear surface elements were used. Once the velocity of the surface elements is known, then their position at a later time can be determined through the integration of equation (12) by quadratures. The code as developed is capable of determining the free surface evolution for any given initial geometry by marching the solution with time. The code was validated by repeating some of the results given in reference [13].

Figures 1 and 2 show the results from the numerical computation for the evolution of the coalescence process of two infinitely long cylinders under the influence of the capillary force alone. Figure 1 shows the shape evolution for two cylinders with equal radii, while figure 2 shows the shape evolution for two cylinders with different radii in which the radius of one cylinder is twice the other. The final equilibrium shape in both cases leads also to an infinitely long circular cylinder which is in agreement with the minimum energy principle in the absence of the force of gravity or other body forces.

B. Axisymmetric Geometry

In anticipation of the use of the numerical results in conjunction with experimental measurements, the coalescence of the two dimensional circular cylinders is not of practical interest in here since the experiment is performed using two spherical drops. To this end the analysis described above for rectangular Cartesian coordinate system is modified in the manner described below to enable the simulation of the coalescence process of two spherical drops. This can be easily accomplished by introducing the following transformation from the Cartesian coordinate system (x_1, x_2, x_3) used in the analysis for the two-dimensional case outlined above, to a cylindrical coordinate system (r, θ, z) needed for the spherical geometry (see [14]):

$$x_i = (x_1, x_2, x_3)^T = (r\cos\theta, r\sin\theta, z)^T\,. \tag{13}$$

Since the cylindrical coordinates are functions of all three Cartesian coordinates, then the tensoral functions in (8), namely c_{ij}, q_{ij} and u_{ij} must all be written for i, j = 1, 2, 3 in the following manner:

$$c_{ij}\left\{= \delta_{ij}, \mathbf{x}\in\Omega;\quad = \delta_{ij}/2, \mathbf{x}\in\Gamma;\quad = 0, \mathbf{x}\in\Omega'\right\}; \tag{14}$$

$$q_{ij}(x_i, y_i) = \frac{3(x_i - y_i)(x_j - y_j)(x_\kappa - y_\kappa)n_\kappa}{4\pi|\mathbf{x}-\mathbf{y}|^5}\,, \tag{15}$$

$$s_{ij}(x_i, y_i) = \frac{1}{8\pi}\left[\frac{\delta_{ij}}{|\mathbf{x}-\mathbf{y}|} + \frac{(x_i - y_i)(x_j - y_j)}{|\mathbf{x}-\mathbf{y}|^3}\right]. \tag{16}$$

Where again the position vector $\mathbf{y}$ represents the free surface location, while $\mathbf{x}$ represents an interior point.

In the present analysis axial symmetry will be assumed, i.e. $u_\theta = 0$ such that only u_r and u_z need to be evaluated at the intersection of the surface $\delta\Omega$ with the half-space $\theta = 0$. In this case the intersection curve Γ is such that $\mathbf{x} = \{(R, 0, Z)^T \in \Gamma\}$. After successive substitutions of the cylindrical coordinates in equation (8) and upon integration along the θ-direction, equation (8) takes the following form for cylindrical coordinates:

$$c_{\alpha\beta}u^c_\beta + \int_\Gamma q^c_{\alpha\beta}u^c_\beta d\Gamma = \int_\Gamma s^c_{\alpha\beta}b^c_\beta d\Gamma \tag{17}$$

where the superscript c stands for cylindrical coordinates, and α and β are either 1 or 2 and hence $\mathrm{u}^c = (u^c_1, u^c_2)^T = (u_r, u_z)^T$. The coefficients $q^c_{\alpha\beta}$ and $s^c_{\alpha\beta}$ can be written in terms of complete elliptic integrals of the first and second kind and are given in

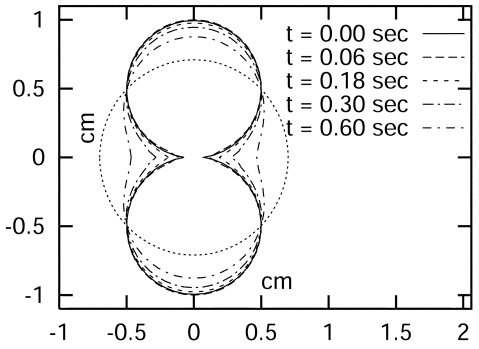

Fig. 1. Time evolution of the coalescence of two liquid cylinders of equal radii.

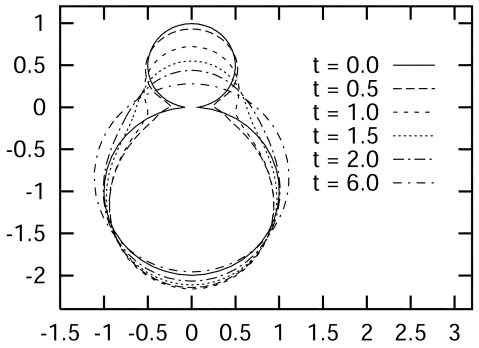

Fig. 2. Same as in Figure 1 but with unequal radii.

detail in [14].

The computer program discussed earlier for the two-dimensional coalescence case was modified to allow it to perform the computations for axisymmetric surfaces in cylindrical coordinates as outlined above. Figure 3 shows the shape evolution resulting from the coalescence of two spherical drops of equal radii. In figure 3 the shape evolution is shown as a function of time, t. Again in here, as in the Cartesian coordinate geometry case, the the final shape takes the form of a spherical drop whose final volume equals the sum of the volumes of the two drops in the absence of any body force.

An important feature of the coalescence processes shown in figures 1 - 3 is the uniqueness of the surface shape evolution as the coalescence proceeds from two volumes (cylinders or spheres) to a final single volume (a cylinder or a sphere). This shape evolution is consistent with the minimum surface energy principle which, for zero gravity, predicts a final shape of a circular cylinder for the two dimensional case, and a sphere for the three dimensional case, [15]. Due to the uniqueness of the terminal geometry of the present coalescence process, it is possible define a single characteristic measure, in this case, which represents the evolution of the coalescence process. A very appropriate measure in this case is the variation of the contact diameter as a function of time as the two volumes merge into a single volume. Figure 4 shows the variation, with time, of the contact radius as two cylinders of equal diameters merge and also as two spheres of equal diameter merge. It should also be noted that the contact radii shown in figure 4 have finite values at time $t = 0$. This was necessary due to the fact that severe numerical difficulties may be encountered if the numerical computations were initiated at the precise time of contact for which case the contact radius is zero in both cases. To avoid such difficulties the computations were always initiated at a finite, but small, value for the contact radius. The smallest contact radius possible in the present computations was of the order $R_c(t = 0) \approx 0.1$. It should be noted that this approach does not introduce errors in the solution whenever it is properly handled. The origin of this problem can be clearly observed in figures 1 - 3 which show the angle between the perimeters of the two circles at the instant of contact is almost zero. The sharper the cusp at the instant of contact the more difficult the numerical approximation becomes.

Figure 4 shows that the two curves, one for two cylinders and the other for two spheres, posses similar variation of the contact radius with time. However, each curve is seen to asymptote to a different value for the contact radius. For the spherical drops case, the asymptotic value for the contact radius is $2^{1/3} = 1.2599$ times the radius of the original drops, while for the two-dimensional case the asymptotic value is $\sqrt{2} = 1.414$ times the original radius. This is as expected, since in the absence of any body force and under the influence of capillary force alone, the two spheres will coalesce into a single sphere whose volume is twice that of the original one, while in the two-dimensional case the two circles will coalesce to a single circle whose area is twice the original one [15].

It is clear from examining the governing equation (2) and the boundary conditions (3) that the evolution of the free surface shape, as the two liquid volumes merge, is dependent upon the only two parameters appearing in these equations, namely the viscosity of the liquid μ and its surface tension σ. Also, due to the uniqueness of the solution given by condition (12), the shape evolution of the free surface curve is also a unique function of the two parameters μ and σ, i.e.

$$\mathbf{x} = \mathbf{x}(t; \mathbf{x}_0, \mu, \sigma), \quad \mathbf{x}_0 = \mathbf{x}(t = 0).$$

In other words, the free surface shape evolution will be different for different values of either μ or σ. Thus, the objective of this analysis is to determine the viscosity of the liquid from the experimentally identified unique shape evolution of two merging liquid volumes of the same fluid under the action of surface tension alone. This is accomplished by comparing the experimentally measured geometry and velocity of the free surface with the numerical solution obtained from equation (17) together with the appropriate values for both the viscosity and the surface tension.

3 Experimental Procedure

A simple experiment was designed, constructed and performed on board the NASA KC-135 aircraft for the purpose of validating the drop coalescence method as means for measuring the viscosity of liquids. The objective of the experiment was to allow two liquid drops to coalesce under the influence of the surface tension force alone during the low gravity segment of the flight parabola. A simple experimental platform capable of being carried on board the NASA KC-135 aircraft was designed and constructed to implement this objective. A sketch of the experimental configuration is shown in figure 5. The experimental apparatus includes a syringe pump used to create the liquid drops, the test cell within which the drop coalescence is performed, and a 16 mm high-speed movie camera for visualizing the coalescence process. The test apparatus also included a tri-axial accelerometer with a digital readout. The test cell was fabricated from transparent plexiglas and is cubical in shape measuring 6.5 cm on each side. Two 13 gauge hypodermic needles were attached on two opposite faces of the test cell on whose tips the drops were supported. The needles were each connected to a separate hypodermic syringe and were driven by the syringe pump. Different size syringes were used to allow for the formation of different size drops. The precision syringe pump was capable of flow rates ranging from 1 μl/min up to 100 ml/min thus allowing the formation of a wide range of sizes of the drops.

Each test was conducted by activating the syringe pump immediately after the low gravity segment of the flight parabola was attained. Once the drops reached their predetermined sizes, they were then brought into contact together manually. Once the drops were touching, the coalescence process was allowed to proceed independently under the influence of the

surface tension force alone by stopping the motion of the needles. The coalescence process was visually recorded using a high speed movie camera. The coalescence process is extremely fast, normally, and for the specific test liquids used, it was achieved in under 1 second. Measurements of the merging process were performed by analyzing several individual film frames from which the free surface velocity was determined, or in this case, the length of the contact radius. It should be emphasized that the experimental procedure described in here was manual for the most part. This is primarily due to the preliminary nature of the experiments and should not be construed as the final measurement technique to be recommended. The final experimental procedure is expected to be mechanized as a result of the experience gained from the tests discussed in here.

The results discussed in the next section are from two flight campaigns which were conducted approximately one year apart. The tests in the first flight campaign were performed for different drop sizes ranging in diameter from 8 to 15 mm, and for different liquids. However, the coalescence process was always performed using two drops from the same liquid. In a subsequent second set of experiments, temperature sensing thermisters were attached to the tips of the needles for the purpose of measuring the liquid temperature during the coalescence process. This was achieved by attaching a thermister at the tip of each needle which were connected to a digital readout designed to be visible in the field of view of the camera. This allowed for recording the temperature of each drop during the coalescence process.

4 Results and Discussion

The kinematics of the free surface evolution during coalescence of two spherical drops can be simulated through an accurate solution to equation (17). As indicated earlier an accurate and robust simulation of the coalescence process can be obtained through a numerical solution to the equation. An analytical solution of the two dimensional problem, i.e. for infinitely long circular cylinders, using complex function analysis is described by Hopper [16, 17]. However, the only possible solution for spherical geometry, such as for two drops, or other more complex geometries must be obtained through numerical means. The analytical simulations of the coalescence process in the results discussed in this section were all produced through numerical solution of the system of equations for spherical drops using the BEM.

A. Low Gravity Test

In the experimental leg of this study four liquids, in all, were used in the first set of tests performed during the first KC-135 flight campaign. These included glycerin, water, and two silicone oils each with a different value for the viscosity. These liquids were chosen to allow for testing a reasonably wide range in both the viscosity and the surface tension values for the experiment at ambient temperature and pressure conditions. The viscosity of the liquids chosen varied by several orders of magnitude while the surface tension coefficient varied by about a factor of three. However, the tests in which the two different silicone oils were used yielded unsatisfactory results due to their undesirable wetting properties and low surface tension values which inhibited the formation and the subsequent deployment of the required drops. The tests using water and glycerin yielded better results since it was possible to deploy reasonably good drops with these liquids which also had the desired size and geometry. However, for the case in which water was the working fluid, the coalescence process was found to be extremely fast, in the order of few milliseconds, which made the analysis of the process extremely difficult taking into account the camera speeds available during these tests. In this case, and since the camera speed was the same for all of the tests performed, of the order of 250 frames/s, the coalescence process of two water drops was completed within few frames only. On the other hand, glycerin gave the best results in the first series of tests conducted on board the KC-135 such that only these results are presented and discussed below.

Figure 6 shows a sequence of 5 successive frames during the merging of two glycerin drops, each 1 cm in diameter. The contact radius was measured in each frame. Also, it was possible to calculate the elapsed time between successive frames from the known film speed used for visualization, namely 250 frames/s in this case. However, there was no general time reference available for use to mark the initiation of the coalescence process which would establish the elapsed time for the first frame in the sequence shown in figure 6. Due to this ambiguity of the time line assumptions had to be made in order to establish the time origin for the first frame shown in fig. 6. Figure 7 shows the measured contact radius variation with time for each frame in Figure 6. The time for the first data point was the best estimate that could be made from other known time line estimates.

Figure 7 also shows the calculated contact radii, R_c, variation with time obtained from the numerical computations in which the appropriate glycerin viscosity value was used corresponding to four different temperatures, 25°, 30°, 35° and 40°C, respectively. Since the viscosity of glycerin is a strong function of temperature as shown in figure 8, [18], it can be seen that the curves appear to be widely separated over this small range of temperatures indicating a significantly large variation in the viscosity values used for constructing these curves. In fact the variation of the viscosity value over the range of temperatures shown is about a factor of 3, ranging from 1.48 Pa s at 20°C to 0.33 Pa s at 40°C, [18]. However, the coefficient of surface tension, σ, varies by no more 1.5% over the same range of temperatures, (.0594 - .0585 N/m, [18]). The dimensional time t^* and contact radius values R_c shown in figure 7 were calculated from their non-dimensional counterparts obtained from the numerical computations by using the appropriate time and length scales in the following manner:

$$t^* = t\,D\mu/\sigma, \quad R_c = D/2$$

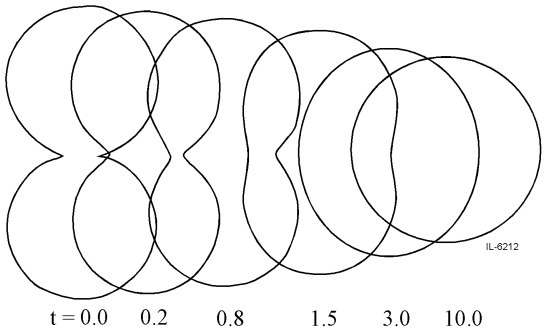

Fig. 3. Time evolution of the coalescence of two spherical drops of equal radii.

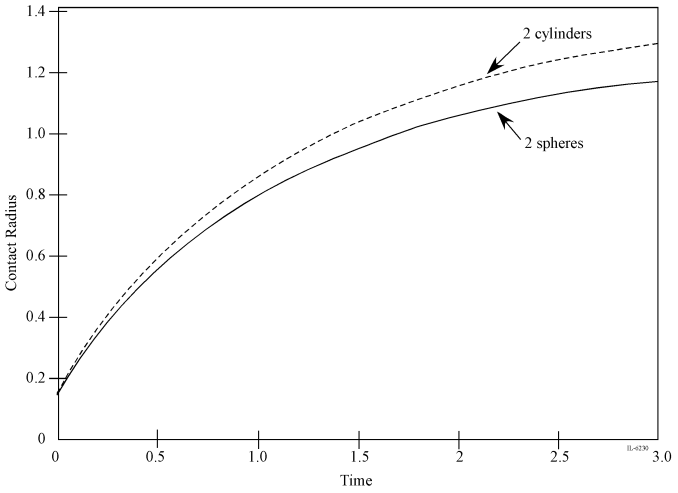

Fig. 4. Time variation of the contact radius during the coalescence of two liquid cylinders and two spheres of equal radii.

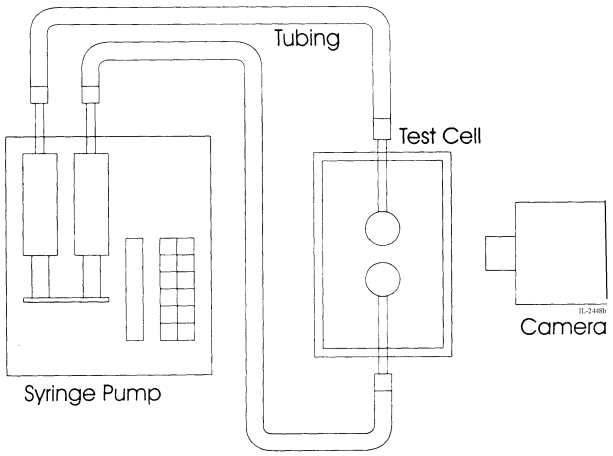

Fig. 5. A schematic of the flight experimental apparatus.

where D is the initial drop diameter and t is the non-dimensional time.

Note, that only five experimental data points are shown in figure 7 which correspond to the measurements obtained from the five frames shown in figure 6. In Figures 7, only the initial stages of the coalescence process are compared with the theoretical calculations since the terminal shape in the experiment evolves into a liquid bridge which is different from the terminal shape in the theory which evolves to a spherical drop. The descrepency in the terminal shapes between the experiment and the theory is due to the fact that the coalescing drops in the experiment had to be constrained while in the theory they were not. The coalescing drops had to be rigidly supported in the experimental apparatus. Due to this disparity in the terminal shape evolution it was not possible to use the experimental data beyond the fifth frame of figure 6 for comparison purposes with the theory. However, it is assumed that the initial stages of the coalescence process proceed almost independent of the final shape and depends only on the initial shape of the drops as the coalescence process progresed. In this case the initial shape of the drops was spherical for both the experiment and the theory. This criterion is used throughout this study.

It is clear from figure 7 that the experimental measurements appear to agree best with the curve for which viscosity value is that corresponding to a glycerin temperature of 37°C. However, since serious ambiguity was encountered in establishing the time reference for the first data point, the same data were replotted in a manner which tended to minimize its dependence on the reference time for the initial data point in the following manner. The time for the smallest experimental contact radius measured was made to coincide with the theoretically computed time at that value of the contact radius appropriate for each glycerin temperature. This time was then used as the initial time for computing the subsequent time for each successive experimentally measured contact radius from the known film speed. The result of such interpretation of the experimental data is shown in figure 9. It is clear from figure 9 that the experimental measurements appear to agree best with the computed curve for glycerin at 35°C. This is basically very close to the value obtained in figure 7. Unfortunately, it was not possible to confirm the exact glycerin temperature during these tests since no provision was made in the experimental apparatus for measuring the temperature of the drops during coalescence. The analysis of the experimental results by either method clearly indicates that the glycerin temperature at the time the tests were performed must have been around 35°C.

The comparison between the theoretically computed contact radius and the measured value in this set of experiments lacks the knowledge of the exact temperature of glycerin during the coalescence process. This ambiguity was not anticipated when the experiment was first devised. Thus in order to assess the relevance of the experimental data to the viscosity measurement objective, the temperature of the test liquid during the test had to be extrapolated. Due to the fact that high speed photography, requiring high intensity illumination, was involved in the tests, and coupled with the prevailing environmental conditions, it seems likely that the liquid temperature was indeed in the range of ~ 35°C. With this in mind, it is quite reasonable to assume that the measured data of figures 7 and 9 do confirm, albeit in a general manner, that the method can be effectively used for

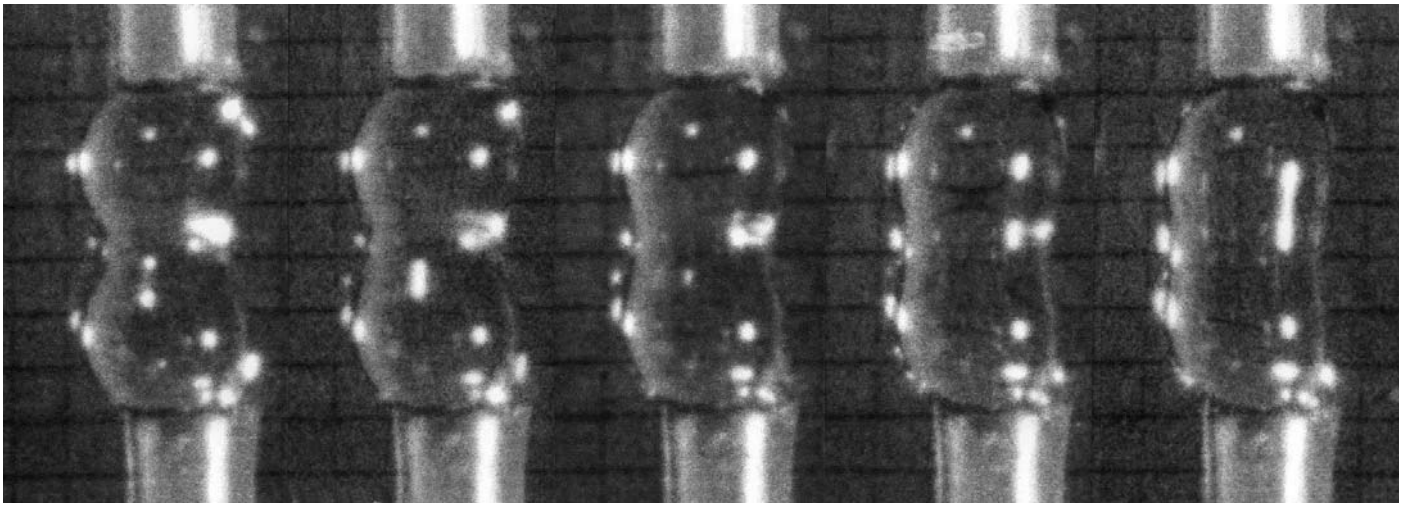

Fig. 6. Five successive frames showing the merging of two liquid drops of equal diameter. Time increasing from left to right.

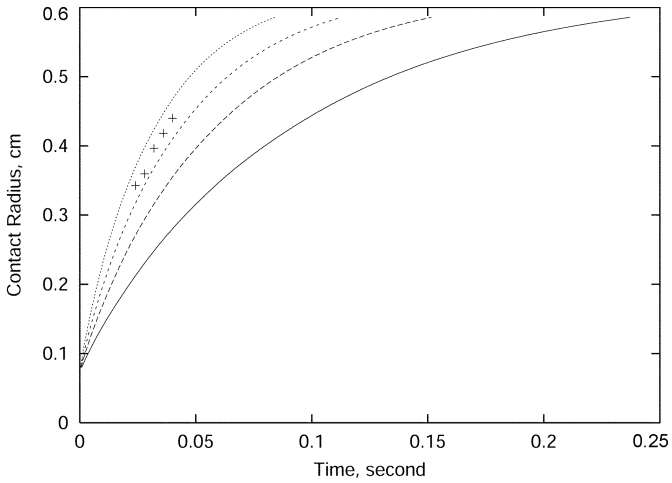

Fig. 7. Measured + + +, and computed contact radius variation with time for glycerine at viscosities corresponding to different temperatures. ——, 25°C; – – –, 30°C; - - -, 35°C; · · ·, 40°C.

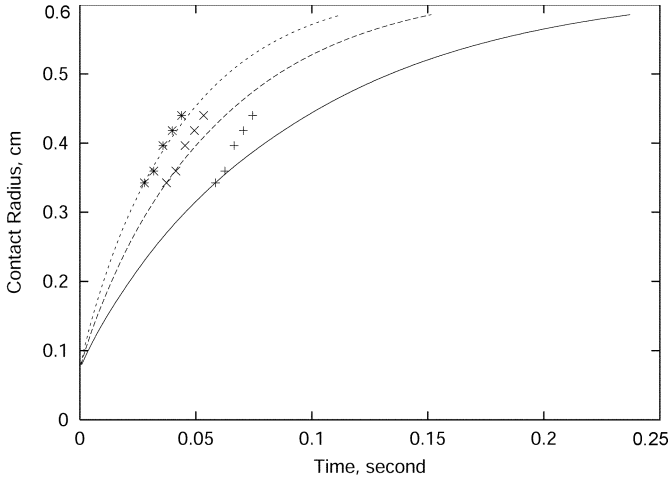

Fig. 9. Measured +, ×, ∗, and computed contact radius variation with time for glycerine at viscosities corresponding to different temperatures. ——, 25°C; – – –, 30°C; - - -, 35°C.

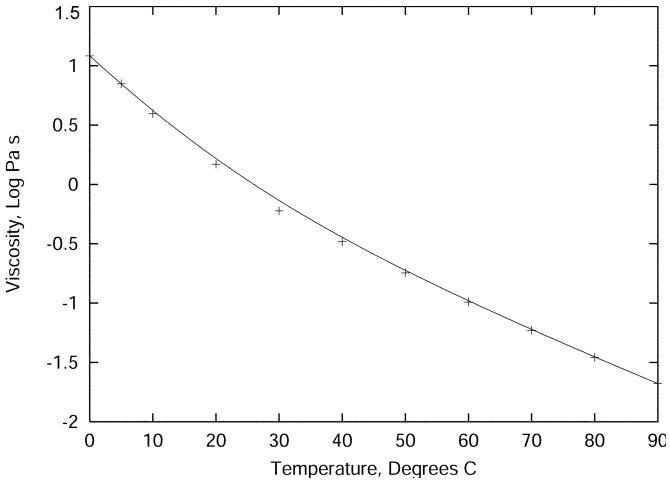

Fig. 8. Glycerin viscosity variation as a function of temperature [18].

measuring liquid viscosity of highly viscous substances. Also, the data shown in figures 7 and 9 appear to be within the experimental error range.

B. Second Low Gravity Test

The fact that the viscosity of glycerin is a very strong function of temperature, shows that the data discussed above for glycerin lack a very important measurement, namely the temperature of the liquid at the time of coalescence. Also, since glycerin viscosity varies considerably over this small range of temperatures, makes it an ideal ambient condition model liquid for validating the method outlined for viscosity measurements. In recognizing that the liquid temperature represents an essential component of the data for glycerin, a second low gravity KC-135 flight experiment was conducted in which the temperature of the liquid drops was measured during the coalescence process. To this end thermisters were attached at the exit tip of each

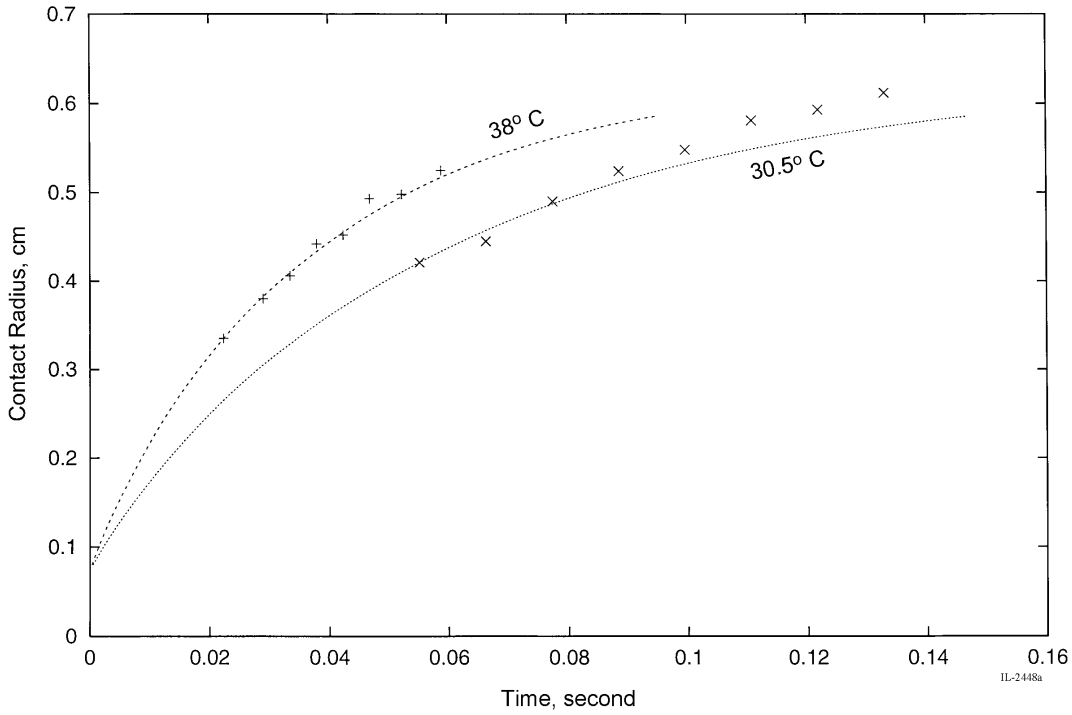

Fig. 10. Measured and calculated contact radius variation with time for two spherical drops of glycerin, each 1 cm diameter, at two temperatures. · · ·, 30.5°C, - - -, 38°C.

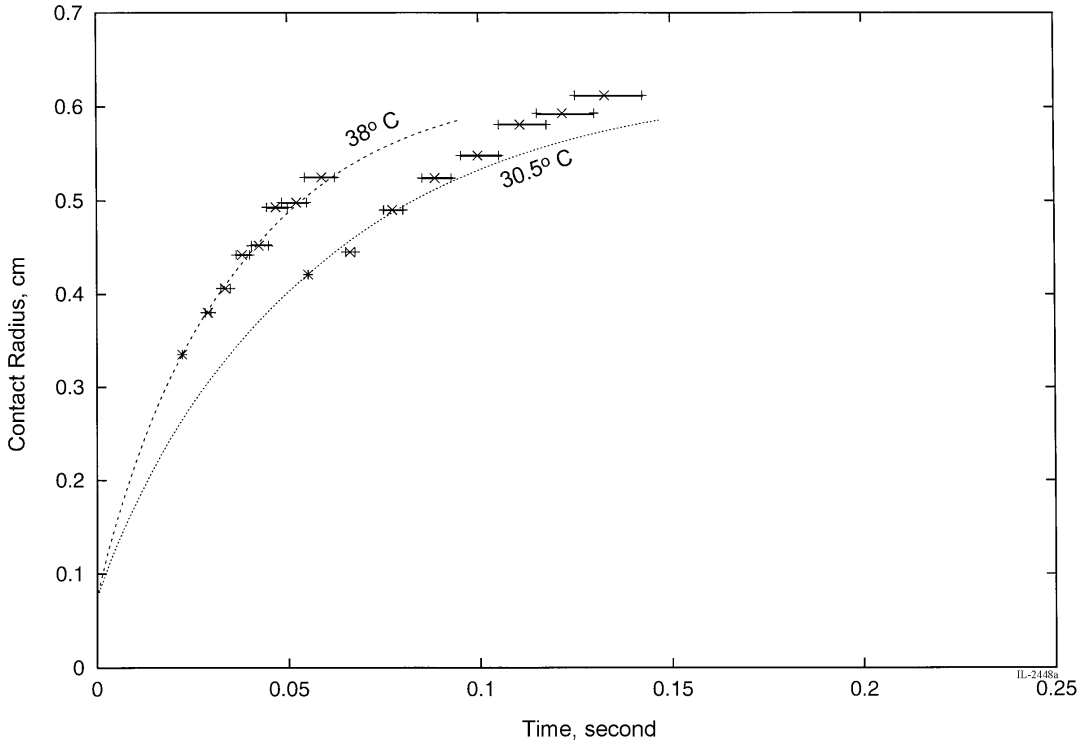

Fig. 11. Same as in 10, but with error bars indicating the measured contact radius at three film speeds of 400, 450, and 500 frames/s.

needle enabling the measurement of the liquid temperature during coalescence. The liquid temperature of each drop was displayed with the aid of a digital readout which was visible within the photographed frames during the coalescence process. This modification of the apparatus allowed for monitoring the temperatures of the drops as they coalesced. Thus, glycerin was the only liquid used in all of the tests conducted during the second KC-135 flight campaign. However, the tests were conducted at different glycerin temperatures ranging from 10°C up to 40°C which allowed for the viscosity to vary by approximately one order of magnitude, as shown in figure 8.

Figure 10 shows the measured contact radius variation with time for two 1 cm diameter glycerin drops at two average temperatures of 30.5° and 38°C, respectively. The experimental data in this figure are compared with the numerically computed contact radius variation with time also for two 1 cm diameter spherical drops in which the appropriate viscosity at the respective temperature was used. Note, that the time for the first contact radius point in each case in this figure was again referenced to the numerically computed time in a manner similar to that displayed in figure 9. The film speed for the tests in this case was increased to a nominal value of 500 frames/s to allow for accumulating greater amount of data. However, the camera speed could not be kept uniform during any single test for all tests throughout the flight. In fact the camera speed was found to vary between 400 and 500 frames/s, due to the acceleration and deceleration of the camera motor during the filming process. The experimental data points in figure 10 are plotted at an average film speed of 450 frames/s. Figure 11 shows the same plot as that of figure 10 except in this case the experimental data were calculated for three film speeds, 400, 450, and 500 frames/s, respectively rather than a single average film speed. The error bars shown in each case are for the upper and lower ranges of the film speed used. Also the temperature for the analytical curves shown in figures 10 and 11 are the average temperatures for the two coalescing drops. These figures show reasonable agreement between the experimental data and the calculated curves in spite of the fact of the numerous experimental sources of error present in these tests. The agreement between the data and the theory appear to be quite good up to a contact radius value of about 0.5. Beyond this contact radius, deviations are observed. This is to be expected since the two drops were constrained in the experiment and could not evolve into a sphere as predicted by the theory but rather they evolved into a short liquid cylindrical bridge.

The results shown in figures 10 and 11 appear to be encouraging in spite of the many constraints imposed in the experimental phase of this study. The experiments were designed to be performed on board the KC-135 in which the low gravity environment is limited to a maximum of 20 seconds with the added complexity of large oscillations in the acceleration environment (g-jitter). However, the major shortcoming of the experimental phase concerns the execution of the coalescence process. The two drops had to be as rigidly suspended as possible in order to avoid separation from their support by the large g-jitter environment and hence the needle tip support, which does not represent an ideal configuration for this test. Second, in order to perform the tests conveniently, the two drops had to be brought together from opposite ends of the test cell, a process far different from the complete coalescence of two freely suspended drops. Nevertheless, in spite of all these major shortcomings, the deviation of the predicted value for the viscosity from its exact value was no more than a few percent.

Concluding Remarks

The results shown in figures 7, and 9 - 11 clearly demonstrate that, in the absence of gravity, there exists good agreement between the measured speed of coalescence, for two spherical drops, and the computed one for the specific value of the liquid viscosity. It is also obvious from the discussion above that the experimental apparatus and procedure is far from perfect and possess many deficiencies. Such shortcomings, however, must be rectified before the method outlined above can be seriously considered for use as means for measuring liquid viscosity. Nevertheless, it has been shown in here that there exists remarkable agreement between theory and experiment which makes the coalescence method an extremely attractive one for measuring the viscosity of highly viscous liquids. Two attributes makes this method a very attractive one. The first concerns the simplicity of the numerical computations involved, while the second is due to the directness of comparison with experiment. The former feature is due to the fact that only the free surface kinetics are considered without the complications involved in accounting for the dynamical effects present under imposed force fields including the force of gravity. Thus, the microgravity environment is essential for the coalescence process in order for this method to a be useful one since the levitation force fields can be eliminated including the acceleration due to gravity. It is obvious that this method is more direct than, and superior to, the method of drop oscillation since the latter requires extensive and complicated computations as well as the use of external force fields necessary for inducing the oscillations. Also, the drop oscillation method can not be used for viscous liquids in the region of undercooling where knowledge of the value of the viscosity is very important for crystallization studies.

It is understood that for this method to be an accurate and a viable technique for measuring liquid viscosity major improvements need to be made to the coalescence process as well as for the data acquisition system. These steps include, ensuring that the initial drop volumes are highly calibrated to be measured within less than one percent. The coalescence process must allow for the two drops to freely coalesce without any mechanical constraints such as the needle tips used in here and without any dynamical forcing. These improvements can be accomplished in microgravity environment with some modification of the design of the test process. For instance, it is always possible to

form as close to a perfect spherical drop in microgravity environment. Also, the two drops can be suspended by a thin wire in microgravity and be made to coalesce by moving the two wires very gently close to each other from the side until they touch and then allowing the two drops to merge as freely as possible and evolve into a single spherical drop. It is strongly believed based on the evidence presented in here that it is possible to measure the viscosity of any liquid with an accuracy in the range of one percent using the method presented in here.

We are in the process of improving the experimental procedure in order for this technique be a viable one for viscosity measurement. Some of the improvements include an automated mechanism for the deployment and movement of the drops. Also, the drops will be made to coalescence from the side rather than facing each other in order to avoid the final bridge formation at the end of the coalescence process. A more accurate photographic method will be used employing a digital camera rather than the analogue one used in the tests described in here. A digital camera will render the image analysis more accurate and straight forward. The inclusion of a time standard in the recorded image is an obvious improvement. Other improvements are also being incorporated.

References

1 *Turnbull, D.:* Under What Gravity Can Glass be Formed? Contemp. Phys., vol. 10, p. 473 (1969).

2 *Gutzov, I., Russel, C., Durschang, B.:* Crystallization of glass Forming Melts Under Hydrostatic Pressure and Shear Stress. J. Material Sc., vol. 32, p. 5405 (1997).

3 *Miani, F., Matteazzi, P.:* Estimation of Viscosity in Undercooled Liquid Metal Alloys. J. Non-Crys. Solids, vol. 143, p. 140 (1992).

4 *Ethridge, E. C.:* Unpublished data (1995).

5 *Trinh, E. H.:* Fluid Dynamics and Solidification of Levitated Drops and Shells. Progress in Astronautics and Aeronautics, Koster J. N. and Sani, R. L. (Eds.), vol. 130, p. 515 (1990).

6 *Lamb, H.:* Hydrodynamics. Cambridge Univ. Press, (1932).

7 *Prosperetti, A.:* Normal-Mode Analysis for the Oscillation of Viscous Liquid Drop in an Immiscible Liquid. J. de Mec., vol. 19, p. 149 (1980).

8 *Lundgren, T. S., Mansour, N. N.:* Oscillation of Drops in Zero Gravity with Weak Viscous Effects. J. Fluid Mech., vol. 194, p. 479 (1988).

9 *Basaran, O. A.:* Nonlinear Oscillation of Viscous Liquid Drops. J. Fluid Mech., vol. 241, p. 169 (1992).

10 *Happel, J., Brenner, H.:* Low Reynolds Number Hydrodynamics. Prentice Hall (1965).

11 *Ladyzhenskaya, O. A.:* The Mathematical Theory of Viscous Incompressible Flow. Gordon & Breach, New York (1963).

12 *Becker, A. A.:* The Boundary Element Method in Engineering. McGraw-Hill (1992).

13 *Vorst van de, G. A. L., Mattheij, R. M. M., Kuiken, H. K.:* A Boundary Element Solution for Two-Dimensional Viscous Sintering. J. Comp. Phys., vol. 100, p. 50 (1992).

14 *Vorst van de, G. A. L., Mattheij, R. M. M.:* Simulation of Viscous Sintering. in B E Applications in Fluid mechanics, H. Power, Ed., Computational Mechanics Publications, Southampton and Boston, p. 215 (1995).

15 *Antar, B. N., Nuotio-Antar, V. S.:* Fundamentals of Low Gravity Fluid Dynamics and Heat Transfer. CRC Press, Boca Raton (1993).

16 *Hopper, R. W.:* Coalescence of Two Viscous Cylinders by Capillarity: Part I, Theory. J. Am. Ceram. Soc., vol. 76, p. 1947 (1993).

17 *Hopper, R. W.:* Coalescence of Two Viscous Cylinders by Capillarity: Part II, Shape Evolution. J. Am. Ceram. Soc., vol. 76, p. 2953 (1993).

18 CRC Handbook of Chem. and Phys., 68th edition, CRC Press (1987-1988).